

# Growth, optical and EPR properties of $\text{Li}_{1.72}\text{Na}_{0.28}\text{Ge}_4\text{O}_9$ single crystals pure and slightly doped with $\text{Cr}^{3+}$

Research Article

Anna Jasik<sup>1†</sup>, Marek Berkowski<sup>2</sup>, Sławomir M. Kaczmarek<sup>1</sup>, Andrzej Suchocki<sup>2,3</sup>, Agata Kaminska<sup>2</sup>, Grzegorz Leniec<sup>1</sup>, Piotr Nowakowski<sup>2</sup>, Viktor Domukhovski<sup>2</sup>

<sup>1</sup> Institute of Physics, Faculty of Mechanical Engineering and Mechatronics, West Pomeranian University of Technology, Al. Piastów 48, 70-311 Szczecin, Poland

<sup>2</sup> Institute of Physics, Polish Academy of Sciences, Al. Lotników 32/46, 02-668 Warsaw, Poland

<sup>3</sup> Institute of Physics, Kazimierz Wielki University, ul. Weyssenhoffa 11, 85-072 Bydgoszcz, Poland

Received 29 September; accepted 24 November 2011

## Abstract:

Single crystals of lithium-sodium-tetragermanate, a member of the solid solution series  $\text{Li}_{2-x}\text{Na}_x\text{Ge}_4\text{O}_9$  with  $x=0.28$ , pure and slightly doped with  $\text{Cr}^{3+}$  ions (0.03 mol.% and 0.1 mol.%), were grown in ambient atmosphere by the Czochralski technique from stoichiometric melt. The crystals with dimensions up to 20 mm in diameter and 50 mm in length were obtained. The crystal structure has been determined by means of X-ray diffraction. Phase analysis and structural refinement of the  $\text{Li}_{1.72}\text{Na}_{0.28}\text{Ge}_4\text{O}_9$  crystals were performed by X-ray powder diffraction using Ni-filtered  $\text{Cu } K\alpha$  radiation with a Siemens D5000 diffractometer. The absorption, excitation and photoluminescence spectra of the crystals were measured in the UV-VIS and IR range at low temperatures. EPR investigations were performed using a conventional X-band Bruker ELEXSYS E 500 CW-spectrometer operating at 9.5 GHz with 100 kHz magnetic field modulation. Temperature and angular dependences of the EPR spectra of the crystal samples were recorded in the 3-300 K temperature range.

**PACS (2008):** 42.; 42.55.-f; 42.70.-a

**Keywords:** EPR • single crystal • photoluminescence • Czochralski • crystal growth

© Versita Sp. z o.o.

## 1. Introduction

Single crystal of lithium-sodium-tetragermanate  $\text{Li}_{1.72}\text{Na}_{0.28}\text{Ge}_4\text{O}_9$  is a member of the solid solution series  $\text{Li}_{2-x}\text{Na}_x\text{Ge}_4\text{O}_9$  with  $x=0.28$ . At room temperature, the unit cell of the crystal is orthorhombic with a space

<sup>†</sup>presented at the 3rd International Workshop on Advanced Spectroscopy and Optical Materials, July 17-22, 2011, Gdańsk, Poland

<sup>†</sup>E-mail: anna\_jasik@tlen.pl

group  $D_{2h}^8$ -Pcca [1]. The crystal structure consists of  $[\text{GeO}_3]_n$ -chains of tetrahedrally coordinated Ge-atoms that are connected by  $[\text{GeO}_6]$  octahedral into a three-dimensional network. The low-temperature structure belongs to the orthorhombic space group  $C_{2h}^5$ -P1ca with  $Z=4$  [2, 3]. Alkali metal atoms (Li and Na) are disordered between two equivalent positions (8(f), 4(c)) inside the channels formed by GeO polyhedra. Trivalent chromium ions enter at octahedral Ge position in  $[\text{GeO}_6]$  [3]. The crystal is interesting due to nonlinear dielectric properties. The temperature of ferroelectric phase transition,  $T_c$ , depends on  $x$  and changes from about 110 K for lithium-sodium-tetragermanate  $\text{LiNaGe}_4\text{O}_9$  (LNG) to about 320 K for  $x = 0.2$ . In the range  $0 \leq x \leq 0.2$  the solid solution seems to be a two-phase system and it is not possible to obtain a single crystal [4]. The change in  $T_c$  value may be also reached by doping of LNG crystal with e.g. chromium ions. To analyze the influence of the doping with chromium, EPR technique is usable. In the EPR study of very similar  $\text{Li}_2\text{Ge}_7\text{O}_{15}$ :Cr crystals a model according to which  $\text{Cr}^{3+}$  ions at the  $\text{Ge}^{4+}$  positions, and,  $\text{Li}^+$  interstitial ions compensating an excess of charge, form  $\text{Cr}^{3+}$ - $\text{Li}^+$  pair centres with electric dipole moments aligned parallel to the  $a$  axis, has been reported [5]. The formation of  $\text{Cr}^{3+}$ - $\text{Li}^+$  pair centers implies a sufficiently strong distortion of the crystal field around paramagnetic ions. In particular, this can lead to a considerable change in the phase transition temperature. In this paper we analyze growth conditions for LNG pure and doped with  $\text{Cr}^{3+}$  ions. Substitution of Ge ions by Cr is investigated using EPR and optical (absorption, excitation, photoluminescence) techniques.

## 2. Experimental setup

### 2.1. Crystal growth

Single crystals of  $\text{Li}_{2-x}\text{Na}_x\text{Ge}_4\text{O}_9$  with starting compositions  $x = 0.28$ , pure and doped with Cr, were grown by the Czochralski method in an inductively heated platinum crucible under ambient pressure in the air. The mixture of  $\text{Li}_2\text{CO}_3$ ,  $\text{Na}_2\text{CO}_3$ ,  $\text{GeO}_2$  and  $\text{Cr}_2\text{O}_3$  or  $\text{MnO}$  powders of 99.99% purity were used as starting materials. They were heated at 300°C for 4 hours before weighing, mixing in stoichiometric ratios and melting. The admixture of chromium was doped into the above mixture at the content of 0.03 and 0.1 at.% in place of germanium. The first single crystal was grown on a platinum wire. Next crystals were grown with a flat crystal melt interface on  $\bar{1}010\bar{C}$  oriented seed, with pulling rate of 0.75 mm/h and speed of rotation  $\sim 5$  rpm. The crystals with dimensions up to 20 mm in diameter and 50 mm in length were obtained. Transpar-

ent and almost colourless crystals (only crystals with 0.1 mol.% of Cr have light brown-yellow colour) with tendency to cracking parallel to the cleavage plane (010) and with 20 mm in diameter were grown from 50 mm crucible.

### 2.2. Optical measurements

Polished plates of the crystals, cut perpendicularly to "a" direction with the thickness of 1050  $\mu\text{m}$  were used for optical measurements. The absorption of the crystals was measured with the use of Cary 5000 spectrophotometer with resolution of 0.25 nm in the range of 200–3200 nm. To measure photoluminescence (PL), Solar CM 2203 spectrofluorimeter was applied with resolution of 1 nm in the range of 350–820 nm, and the excitation at 230 nm, 280 nm and 415 nm. The measurements of excitation spectra were performed in the range of 220–600 nm at the emission of  $\lambda_{em}=695$  nm (peaks corresponding to excitation wavelength of 230, 280, 415 and 597 nm).

### 2.3. Structure determination

Phase analysis and structural refinement of the  $\text{Li}_{2-x}\text{Na}_x\text{Ge}_4\text{O}_9$  crystals with starting compositions  $x = 0.28$  were performed by X-ray powder diffraction using Ni-filtered  $\text{Cu K}\alpha$  radiation with a Siemens D5000 diffractometer. Experimental data were collected in the angle range  $20^\circ \leq 2\theta \leq 120^\circ$  with a step of  $0.02^\circ$  and averaging time of 10 s/step. The powder diffraction patterns were analyzed by the Rietveld refinement method.

### 2.4. EPR measurements

The electron paramagnetic resonance (EPR) spectra were recorded on a conventional X-band Bruker ELEXSYS E 500 CW-spectrometer operating at 9.5 GHz with a 100 kHz magnetic field modulation. The investigated samples were well oriented cuboids cut from a single crystal. The first crystal absorption spectra derivative was recorded as a function of the applied magnetic field. The EPR spectra temperature dependence in the 3–300 K temperature range was registered using an Oxford Instruments ESP helium-flow cryostat. All the registered EPR spectra of the investigated complexes were simulated using the EPR-NMR computer program in order to study the spin-Hamiltonian parameters [6].

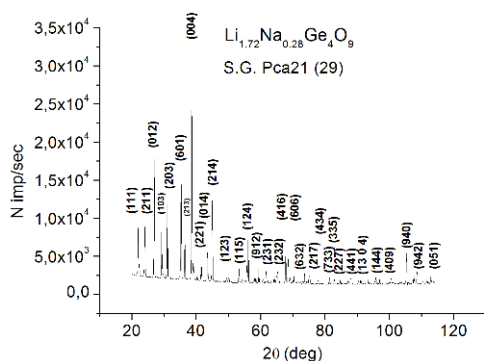


**Figure 1.** X-ray powder diffraction pattern of pure  $\text{Li}_{1.72}\text{Na}_{0.28}\text{Ge}_4\text{O}_9$  single crystal.

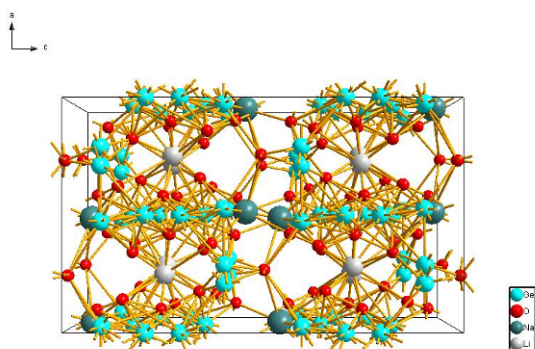


**Figure 2.** Crystal structure of  $\text{Li}_{1.72}\text{Na}_{0.28}\text{Ge}_4\text{O}_9$ .

## 3. Results and discussion

### 3.1. Crystal growth and structure

For the case of  $\text{Li}_{2-x}\text{Na}_x\text{Ge}_4\text{O}_9$  crystal with a decreasing  $x$  value, the volume of unit cell also decreases. This is as estimated by the X ray diffraction data from the literature and Vegard's law. Structure measurements on samples cut from top and bottom of the crystals exhibit decrease in cell volume along the crystal growth direction. In Fig. 1 diffractogram of the  $\text{Li}_{1.72}\text{Na}_{0.28}\text{Ge}_4\text{O}_9$  pure single crystal is presented. The X-ray measurements shows that at the room temperature (RT) the orthorhombic  $D_{2h}^8$ -Pcca unit cell with the lattice parameters  $c=9.3191 \text{ \AA}$ ,  $b=4.6486 \text{ \AA}$  and  $a=15.8410 \text{ \AA}$ ,  $V=686.244 \text{ \AA}^3$  contains four formula units ( $Z=4$ ). In Fig. 2 one can see the structure of  $\text{Li}_{1.72}\text{Na}_{0.28}\text{Ge}_4\text{O}_9$  ( $x=0.28$ ) crystal build up using Diamond 3 program.

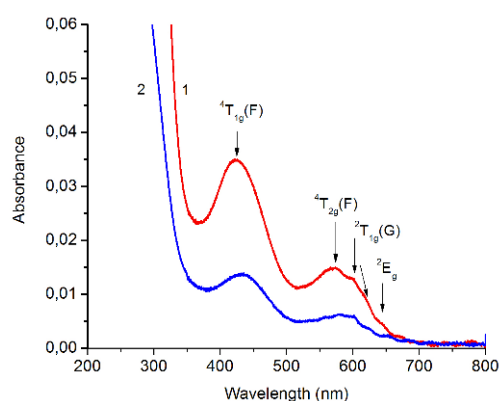


**Figure 3.** RT absorption spectra of two  $\text{Li}_{1.72}\text{Na}_{0.28}\text{Ge}_4\text{O}_9$  single crystals doped with 0.03 mol.% (2) and 0.1 mol.% Cr (1).

### 3.2. Optical properties

#### 3.2.1. Absorption

$\text{Cr}^{3+}$  ions (ionic radius,  $r=62 \text{ pm}$ ) can be substituted in the network presented in Fig. 2 primarily at the octahedral ( $r=54 \text{ pm}$ ) position of germanium ( $\text{Ge}^{4+}$ ) and for tetrahedral positions of germanium at  $r=40 \text{ pm}$ . Due to the small ionic radii difference between  $\text{Ge}^{4+}$  and  $\text{Cr}^{3+}$  ions, we could observe some distortion of the chromium ion environment. Moreover, substitution of the  $\text{Cr}^{3+}$  ion at  $\text{Ge}^{4+}$  site requires charge compensation, which may be realized by interstitial position of  $\text{Li}^+$  or  $\text{Na}^+$  ions in the neighborhood of  $\text{Cr}^{3+}$  dopant; the former is diamagnetic and the latter is paramagnetic. Thus  $\text{Cr}^{3+}\text{-Li}^+$  and  $\text{Cr}^{3+}\text{-Na}^+$  pairs may exist in the  $\text{LiNG:Cr}^{3+}$  single crystal, changing some physical properties of the crystal. Introduction of the compensating ion in the neighborhood of  $\text{Cr}^{3+}$  ion leads to a reduction of its local symmetry, so the paired chromium centers may be of  $C_2$  or lower local symmetry. Electron configuration of  $\text{Cr}^{3+}$  ground state ( $3d^3$ ) involves the free-ion multiplets  $^4F$ ,  $^4P$ ,  $^2G$ , and a number of additional doublet states out of which the ground state is  $^4F$ . There are  $^4A_{2g}$ ,  $^2E_g$ ,  $^2T_{1g}$  and  $^2T_{2g}$  states in the octahedral environment for strong fields (configuration  $(t_{2g})^3$ ).  $^4A_{2g}$  state is lowest and constitutes a ground state of  $\text{Cr}^{3+}$  ion. The first excited state configuration  $((t_{2g})^2(e_g)^1)$  includes three states  $^4T_{1g}(F)$ ,  $^4T_{2g}(F)$  and  $^4T_{1g}(P)$ , and a number of doublet states. In weak field  $^4F$  splits into  $^4A_{2g}(F)$ ,  $^4T_{2g}$  and  $^4T_{1g}(F)$  while  $^4P$  gives  $^4T_{1g}(P)$ . Among the doublet states,  $^2G$  splits into  $^2A_{1g}(G)$ ,  $^2E_g(G)$ ,  $^2T_{1g}(G)$  and  $^2T_{2g}(G)$ , whereas  $^2H$  gives  $^2E_g(H)$ ,  $^2T_{1g}(H)$  and  $^2T_{2g}(H)$ . Low-field terms  $^4A_{2g}(F)$ ,  $^2E_g(G)$ ,  $^2T_{1g}(G)$  and  $^2T_{2g}(G)$  correspond to the lowest strong field configura-

tion  $t_{2g}^3, {}^4A_{2g}(F)$  is a ground state for any crystal field strange. Therefore, there are only two spin-allowed transitions,  ${}^4A_{2g}(F) \rightarrow {}^4T_{2g}(F)$  and  ${}^4A_{2g}(F) \rightarrow {}^4T_{1g}(F)$ , next to several spin-forbidden transitions. When the symmetry is lowered, the degeneracy of energy level may be lifted and appear some additional absorption states [7]. The room temperature (RT) absorption spectra of  $\text{Li}_{1.72}\text{Na}_{0.28}\text{Ge}_4\text{O}_9$  crystal doped with chromium, with concentrations of 0.03 and 0.1 mol.%, illustrated in Fig. 3. Two intense bands with a maximum at 17532 and 23657  $\text{cm}^{-1}$  and a number of weaker at 16590, 14858, 14245, 13495, 12893  $\text{cm}^{-1}$  are observed. The two intense bands correspond to  ${}^4A_{2g}(F) \rightarrow {}^4T_{2g}(F)$  and  ${}^4A_{2g}(F) \rightarrow {}^4T_{1g}(F)$  electronic transitions, respectively. The first of weaker bands corresponds to the  ${}^4A_{2g}(F) \rightarrow {}^4T_{1g}(G)$  transition, while the other four bands correspond to the spin-forbidden transitions. The value of crystal field splitting parameter,  $Dq$ , and Racah repulsion parameter,  $B$ , were estimated by analyzing the absorption spectra shown in Fig. 3. [9–11]. The intense absorption band with a maximum frequency  $\nu_1=17532 \text{ cm}^{-1}$  corresponding to the  ${}^4A_{2g}(F) \rightarrow {}^4T_{2g}(F)$  transition gives a value of  $10Dq$ . A wave number for the  ${}^4A_{2g}(F) \rightarrow {}^4T_{1g}(F)$  transition is  $\nu_2=23657 \text{ cm}^{-1}$ . The value of  $B$  was estimated to be equal to  $590 \text{ cm}^{-1}$ , which is much lower than for the free ion  $\text{Cr}^{3+}$ ,  $B_{free}=918 \text{ cm}^{-1}$  [11]. This difference may be due to the participation of ionic (besides covalency) bonds between the central ion and ligands. Racah parameter was calculated to be  $C=3548 \text{ cm}^{-1}$ . The resulting value of  $Dq/B=2.97$  is higher than the corresponding values for  $\text{Al}_2\text{O}_3:\text{Cr}$  (2.8 [12]), providing that the  $\text{Cr}^{3+}$  ions in  $\text{Li}_{1.72}\text{Na}_{0.28}\text{Ge}_4\text{O}_9:\text{Cr}$  crystal are in a strong crystalline field. While performing calculations of the absorption coefficient from the transmission spectra it was found that the index of refraction was 1.97, the width of the energy gap was  $E_g=5.27 \text{ eV}$ , and, the fundamental absorption edge (FAE) was equal to 235 nm. FAE shift is 230 nm for chromium doped crystals.

### 3.2.2. PL spectra

A typical excitation and photoluminescence spectra of  $\text{Li}_{1.72}\text{Na}_{0.28}\text{Ge}_4\text{O}_9:\text{Cr}^{3+}$  (0.03 mol.%) crystal at room temperature are presented in Figs. 4a, 4b.

The excitation spectrum contains three clear bands (see Fig. 4a). The absorption edge occurs at 235 nm. The band with a maximum at 275 nm corresponds to the  ${}^2A_{1g}(G)$  level, the band at 423 nm can be attributed to  ${}^4T_{1g}(F)$ , while at 570 nm to  ${}^4T_{2g}(F)$ . Fig. 4b shows the emission spectrum with doublet at 694 nm ( $14409 \text{ cm}^{-1}$ ) and 707 nm ( $14144 \text{ cm}^{-1}$ ). This doublet, intense lines R1 (707 nm) and R2 (694 nm) is characteristic of  $\text{Cr}^{3+}$  ions and is caused by the spin-forbidden transition  ${}^2E_g \rightarrow {}^4A_{2g}$ . Weaker and broader sidebands are obviously phonon tran-

sitions. Phonon sidebands are typical for PL spectra in a case of strong crystal field and reported in many papers for ions of  $d^3$  configuration. In the case of strong crystal field ( $Dq/B=2.97$  for  $\text{LNG}:\text{Cr}$ ) we could not expect broad luminescence bands because first excited state is  ${}^2E$  level and weakly coupled with the lattice. In addition to these bands, the broad luminescence band for the  ${}^4T_{2g}(F) \rightarrow {}^4A_{2g}(F)$  transition is visible. Figs. 5a, b shows the excitation and PL spectra of  $\text{Li}_{1.72}\text{Na}_{0.28}\text{Ge}_4\text{O}_9:\text{Cr}^{3+}$  (0.1 mol.%) crystal. As one can see the excitation bands are the same, but their relative intensity a something different. From Fig. 5b one can conclude that all of three excitation bands, clearly observed in the excitation spectrum, contribute to the emission of chromium ions.

For a different look at the PL spectrum of this crystal at low temperatures see Figs. 6a–c.

At room temperature the emission spectrum at for  $T = 30 \text{ K}$  in Fig. 6a one can distinguish five peaks. These peaks can be assigned to different chromium centers or attributed to Stark effect. One can conclude that the suppression of thermal vibrational energy is due to the decrease in the temperature. The former reason of many PL peaks confirms EPR measurements presented in form of roadmap in Fig. 9. The number of peaks offering PL spectrum changes depends on temperature (Fig. 6b, five at 30 K and 3 for 300 K), suggesting the presence of ferroelectric phase transition in the  $\text{LNG}:\text{Cr}$  crystal. It takes place in the temperature range above 250 K. As one can see from Fig. 6b the intensity of the spectra decreases and their position shifts towards higher wavelengths with increasing temperature, but broadening of the spectra is not a crucial feature. We have measured electric permittivity and found that the ferroelectric phase transition takes place in the crystal at about 259 K, but is strongly anisotropic, being observed mainly in “c” oriented  $\text{LNG}:\text{Cr}$  samples. So, in “a” plates we investigated for optical measurements, it may be not clearly recognizable. Nevertheless, Fig. 6b confirm the conclusion on ferroelectric phase transition above 250 K. Next confirmation we obtained from decay lifetime measurements performed for two of five peaks seen in Fig. 6a, labeling them: peak 2 and peak 3 (see Figs. 6a–c). In Fig. 7 a,b the results of luminescence decay time measurements for two different temperatures are shown, made for two different centers, where the issues are marked in Fig. 6a as peak 2 and peak 3. As one can see these centers have different luminescence decay times that clearly depend on temperature. For peak No. 2 the decay time varies from 3.1 ms (60 K) to 2.5 ms (200 K). For peak No. 3 the decay time varies with temperature from 5.2 ms (60 K) to 3.5 ms (200 K). These times are much shorter than recorded for  $\text{YAG}:\text{Cr}^{3+}$  crystal, for which, in the same temperature range, the luminescence decay time

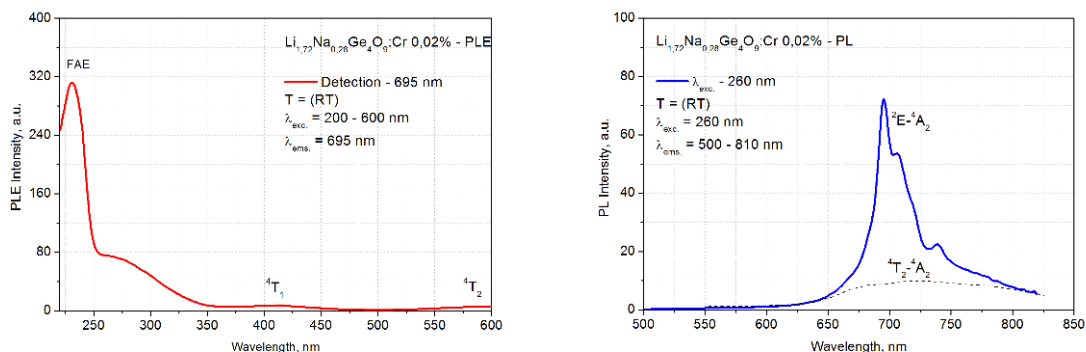


**Figure 4.** (a) PLE spectrum ( $\lambda_{em}=695$  nm), (b) PL spectrum of  $\text{Li}_{1.72}\text{Na}_{0.28}\text{Ge}_4\text{O}_9:\text{Cr}^{3+}$  (0.03 mol.%) single crystal at RT; dashed line - broad  ${}^4\text{T}_2\text{-}{}^4\text{A}_2$  transition.

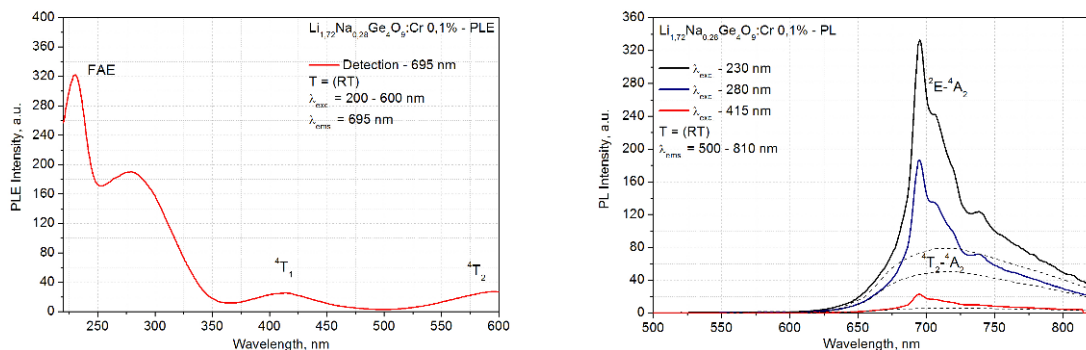


**Figure 5.** (a) RT PLE spectrum ( $\lambda_{em}=695$  nm), (b) RT PL spectrum of  $\text{Li}_{1.72}\text{Na}_{0.28}\text{Ge}_4\text{O}_9:\text{Cr}^{3+}$  (0.1 mol.%) single crystal; dashed lines - broad  ${}^4\text{T}_2\text{-}{}^4\text{A}_2$  transition.

varies within 10 ms to 5 ms [13].

### 3.3. EPR properties

Chromium  $\text{Cr}^{3+}$  ion has an electron spin  $S = 3/2$  and nuclear spin  $I = 3/2$  or 0. The EPR spectrum of the ion originates from odd isotope  ${}^{53}\text{Cr}$  (9.54% abundance) and group of even isotopes  ${}^{50}\text{Cr}$ ,  ${}^{52}\text{Cr}$ ,  ${}^{54}\text{Cr}$  (90.46% abundance) [14]. Our EPR spectrum, due to the lack of hyperfine structure lines, we assigned to the even isotopes. Fourfold degeneracy of the ground state of  $\text{Cr}^{3+}$  ion ( $3/2, {}^4\text{F}$ ) is completely removed in the presence of an external magnetic field. Based on the analysis of the literature we know that the chromium ions in various matrices may give signals described by Zeeman splitting parameter  $g$  with values: 5.37, 4.53, 3.82, 2.26 (isolated) and 1.95–1.98 (pairs, [15, 16]). For some powders there are also observed weak

EPR lines in high fields ( $\sim 600$  mT) [17]. For any randomly chosen  $\text{Li}_{1.72}\text{Na}_{0.28}\text{Ge}_4\text{O}_9:\text{Cr}$  (0.1 mol.%) crystal orientation (Fig. 8), in the EPR spectrum both sharp and intense (low field) and weak, fuzzy (high field) EPR lines are observed. The former are attributed to the differently oriented positions of isolated  $\text{Cr}^{3+}$  ions or  $\text{Cr}^{3+}\text{-Li}^+$  pairs. These items can be traced in three orthogonal planes  $ab$ ,  $bc$  and  $ca$  by drawing the appropriate angular dependences. Magnetically non-equivalent positions for  $\text{Cr}^{3+}$  ions we expect at least one, if not the fifth (as it results from optical investigations). High field lines can be attributed to  $\text{Cr}^{3+}\text{-Na}^+$  pairs or to uncontrolled admixture of rare earth (the lines vanish at 14 K). Thus, the observed EPR spectrum can be described by the following Spin Hamiltonian:

$$H = H_{iso} + H_{pair}, \quad (1)$$

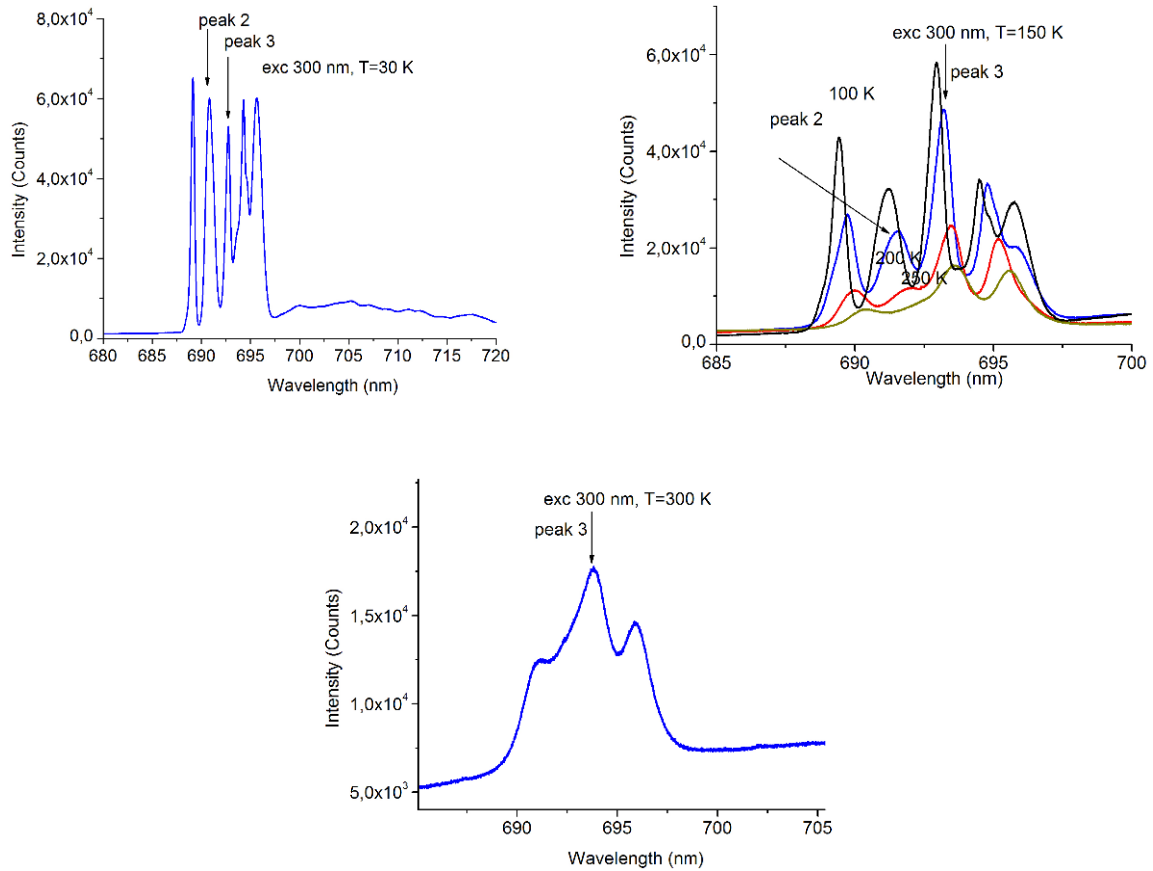


Figure 6. (a) PL spectrum of  $\text{Li}_{1.72}\text{Na}_{0.28}\text{Ge}_4\text{O}_9:\text{Cr}^{3+}$  (0.1 mol.%) single crystal at 30 K, (b). T=150 K, (c). T=300 K.

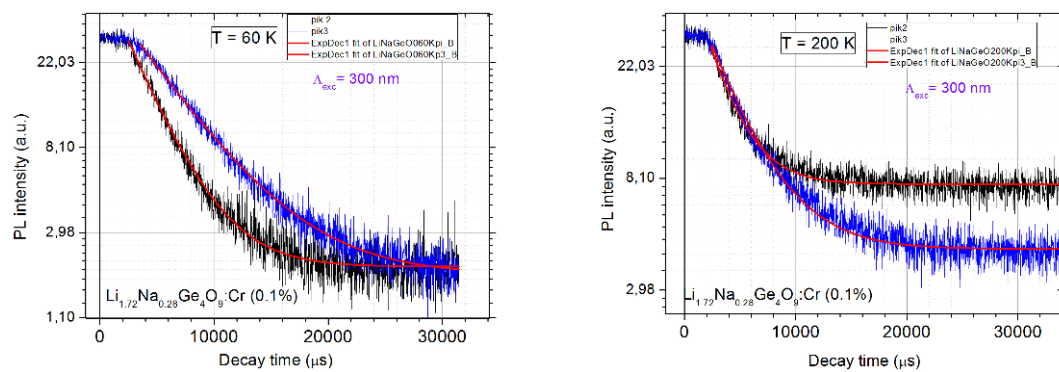
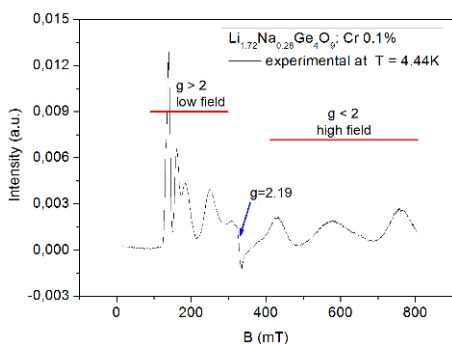


Figure 7. Decay time of PL for the  $\text{Li}_{1.72}\text{Na}_{0.28}\text{Ge}_4\text{O}_9:\text{Cr}^{3+}$  (0.1 mol.%) crystal, for the two centers (peak 2, peak 3) (a). T=60 K i (b). T=200 K.



**Figure 8.** EPR spectrum of  $\text{Li}_{1.72}\text{Na}_{0.28}\text{Ge}_4\text{O}_9:\text{Cr}$  (0.1 mol.%) crystal measured at  $T=4\text{K}$ .

where

$$\begin{aligned} H_{iso} = & \sum_i g_i \beta B S_i + \sum_i D_i [S_{zi}^2 - \frac{1}{3} S(S+1)] \\ & + \sum_i E_i (S_{xi}^2 - S_{yi}^2) \end{aligned} \quad (2)$$

is the Hamiltonian for the isolated chromium ions or  $\text{Cr}^{3+}$ - $\text{Li}^+$  pairs,  $\beta$  is Bohr magneton,  $g$  - Zeeman splitting factor,  $B$  - magnetic field,  $S$  - the spin operator,  $D$  - electron quadrupole matrix; the  $D_i$  - axial and  $E_i$  - rhombic distortion of octahedral (the fine structure parameters of  $i$ -th chromium ion).

$$\begin{aligned} H_{pair} = & \beta B \cdot g^A \cdot S^A + \beta B \cdot g^B \cdot S^B \\ & - 2J S^A \cdot S^B + S^A \cdot D_{dd}^{AB} \cdot S^B \end{aligned} \quad (3)$$

$$D_{dd}^{AB} = \frac{\mu^A \cdot \mu^B}{R^3} - \frac{3(\mu^A \cdot R)(\mu^B \cdot R)}{R^5}, \mu^{A,B} = \beta g^{A,B} \cdot S^{A,B} \quad (4)$$

is the Hamiltonian of ion pairs (e.g. two coupled  $\text{Cr}^{3+}$  ions in positions A and B), where the first two elements are Zeeman elements, the third is the isotropic part of exchange interactions, and the fourth is the magnetic dipole-dipole interaction.

For the  $d^3$  ion such as  $\text{Cr}^{3+}$ , zero-field splitting term originates from interactions of the  $S = 3/2$  spin system with non-cubic component of a ligand field (through spin-orbit coupling). In a  $\text{Li}_{1.72}\text{Na}_{0.28}\text{Ge}_4\text{O}_9:\text{Cr}$  (0.1 mol.%) crystal,  $\text{Cr}^{3+}$  ion environment is approximately octahedron composed of oxygen ions. The value of the zero field constant,  $D$ , suggests on how the position of  $\text{Cr}^{3+}$  ion deviates from

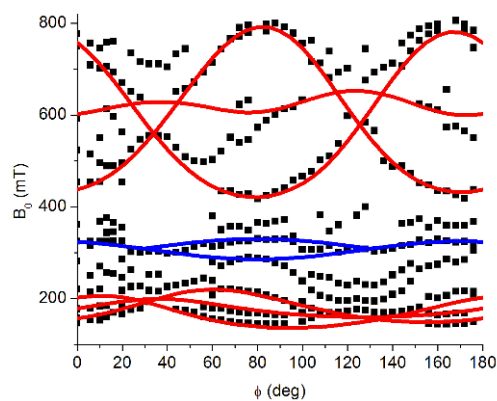


**Figure 9.** The angular dependence of  $\text{Li}_{1.72}\text{Na}_{0.28}\text{Ge}_4\text{O}_9:\text{Cr}$  (0.1 mol.%) crystal in the  $ac$  plane, at  $T=4.5\text{K}$ .

the ideal octahedral geometry. It seems that the environment of this ion is not exactly octahedral due to the value of the  $D$  parameter (Table 1). Fig. 9 shows the angular dependence of the resonance lines positions for  $\text{Li}_{1.72}\text{Na}_{0.28}\text{Ge}_4\text{O}_9:\text{Cr}$  (0.1 mol.%) crystal in the  $ac$  plane, at a temperature of 4.5 K. Besides experimental points, there are plotted solid lines resulting from fitting procedure applied using the EPR-NMR program. As can be seen, at least three magnetically non-equivalent paramagnetic centres one can recognize: two isolated (or  $\text{Cr}^{3+}$ - $\text{Li}^+$ ,  $\text{Cr}^{3+}$ - $\text{Na}^+$  mixed pairs) centres, one in the low, the other in high fields, and, a pair centre ( $\text{Cr}^{3+}$ - $\text{Cr}^{3+}$ ). Similar conclusions one can derive from an angular dependences drawn in a second  $ab$  and third  $bc$  planes. High field EPR lines disappear at a temperature of 14 K, and for low chromium concentration (below 0.03 mol.%).

By using the EPR-NMR program we performed fittings to find the spin Hamiltonian parameters. The results for  $\text{Li}_{1.72}\text{Na}_{0.28}\text{Ge}_4\text{O}_9:\text{Cr}$  (0.1 mol.%) crystal are collected in Tab. 1.

As can be seen from the table, the spin Hamiltonian parameters of  $\text{Cr}^{3+}$  ions paired with  $\text{Li}^+/\text{Na}^+$  indicate on low,  $C_2$ , local symmetry of chromium ions. For  $\text{Cr}^{3+}$  pair centers the constants of exchange interaction,  $J$ , are very small, and therefore these interactions seem to be very weak.

## 4. Conclusions

$\text{Li}_{1.72}\text{Na}_{0.28}\text{Ge}_4\text{O}_9$  and  $\text{Li}_{1.72}\text{Na}_{0.28}\text{Ge}_4\text{O}_9:\text{Cr}$  (0.03 mol.%, 0.1 mol.%) single crystals are transparent in UV-VIS and IR part of optical spectrum and almost colourless.

**Table 1.** Spin Hamiltonian parameters for isolated chromium centres and pairs of chromium ions calculated for  $\text{Li}_{1.72}\text{Na}_{0.28}\text{Ge}_4\text{O}_9:\text{Cr}$  (0.1 mol%) crystal using EPR-NMR program.

	Cr <sup>3+</sup> ions paired with Li <sup>+</sup> /Na <sup>+</sup>		Cr <sup>3+</sup> pairs
$g_{xx}$	3.9	1.11	2.19
$g_{xy}$	0.47	0.0	0.0
$g_{xz}$	0.06	0.0	0.0
$g_{yy}$	3.88	1.11	2.18
$g_{yz}$	0.18	0.1	0.0
$g_{zz}$	3.67	1.17	2.17
$D_{xx}[\text{Gs}]$	273.76	476.77	173.65
$D_{xy}[\text{Gs}]$	0.004	0.0	0.0
$D_{xz}[\text{Gs}]$	0.006	0.0	0.0
$D_{yy}[\text{Gs}]$	-105.9	-211.9	-105.9
$D_{yz}[\text{Gs}]$	0.01	0.0	0.0
$D_{zz}[\text{Gs}]$	-54.09	84.09	-54.1
$J_{xx}[\text{Gs}]$	-	-	0.007987
$J_{yy}[\text{Gs}]$	-	-	0.001341
$J_{zz}[\text{Gs}]$	-	-	0.003853

Only crystals with 0.1 mol.% of Cr have a light brown-yellow colour. Good optical quality of those single crystals ( $T=80\%$ ) were obtained using the Czochralski method. The value of B is  $590\text{ cm}^{-1}$ , Racah parameter is  $3548\text{ cm}^{-1}$ . The resulting value of  $Dq/B=2.97$  shows that the Cr<sup>3+</sup> ions in  $\text{Li}_{1.72}\text{Na}_{0.28}\text{Ge}_4\text{O}_9:\text{Cr}$  crystal are in a strong crystalline field. For any randomly chosen  $\text{Li}_{1.72}\text{Na}_{0.28}\text{Ge}_4\text{O}_9:\text{Cr}$  (0.1 mol.%) crystal orientation, in the EPR spectrum both sharp and intense (low field) and weak, fuzzy (a high field) EPR lines are observed. They are due to Cr<sup>3+</sup>-Li<sup>+</sup>, Cr<sup>3+</sup>-Na<sup>+</sup> and Cr<sup>3+</sup>-Cr<sup>3+</sup> pairs of constituent ions. Compared to room temperatures, in the emission spectrum of LNG:Cr crystal registered for  $T = 30\text{ K}$ , one can distinguish five peaks, that could be assigned to five different chromium centers or could be due to Stark effect. The number of the centers offering PL spectrum changes depending on temperature, what suggests the presence of ferroelectric phase transition. It takes place in the temperature range above 150 K.

## References

- [1] M. Wada, M. Shibata, A. Sawada, Y. Ishibashi, *J. Phys. Soc. Jpn.* 52, 2981 (1983)
- [2] Y. Iwata, N. Koyano, M. Mashida, M. Wada, A. Sawada, *J. Korean Phys. Soc.* 32, S195 (1998)
- [3] A. Sieradzki, A. Ciüman, J. Komar, *Phase Transit.* 81, 999 (2008)
- [4] R. Cach, I. Cebula, M. D. Volnyanskii, *Phys. Status Solidi B* 241, 998 (2004)
- [5] M. P. Trubitsyn, M. D. Volnyanski, A. Yu. Kudzin, *Phys. Solid State.* 46, 1730 (2004)
- [6] M. J. Mombourquette, J. A. Weil, D. G. McGavin, *EPR-NMR user's manual* (Department of Chemistry, University of Saskatchewan, Saskatoon, SK, Canada, 1999)
- [7] R. Kripal, H. Gowind, S. K. Gupta, M. Arora, *Solid State Commun.* 141, 416 (2007)
- [8] R. J. Peruma Reddy, *Coordin. Chem. Rev.* 4, 73 (1969)
- [9] Y. Tanabe, S. Sugano, *J. Phys. Soc. Jpn.* 9, 753 (1954)
- [10] F. Rasheed, K. P. O'Donnel, B. McCollum, B. Henderson, D. B. Hollis, *J. Phys. Condens. Mat.* 3, 1915 (1991)
- [11] C. E. Moore, *National Bureau of Standard Circular no. 467, vol. 2* (US Government Printing Office, Washington, DC, 1952)
- [12] W. Ryba-Romanowski, S. Golab, W. A. Pisarski, D. Podsiadla, Z. Czaplá, *Chem. Phys. Lett.* 264, 323 (1997)
- [13] J. P. Hehir, M. O. Henry, J. P. Larkin, G. F. Imbusch, *J. Phys. C Solid State* 7, 2241 (1974)
- [14] S. Dhanuskodi, A. P. Jeyakumari, *Mater. Chem. Phys.* 87, 292 (2004)
- [15] V. Singh, R. P. S. Chakradhar, J. L. Rao, J.-J. Zhu, *Mater. Chem. Phys.* 111, 143 (2008)
- [16] B. V. Padlyak, M. Grinberg, T. Lukasiewicz, J. Kisielewski, M. Swirkowicz, *J. Alloy. Compd.* 361, 6 (2003)
- [17] T. Weyhermuller, T. K. Paine, E. Bothe, E. Bill, P. Chaudhuri, *Inorg. Chim. Acta* 337, 344 (2002)